TOPS Interferometry with TerraSAR-X.

Pau Prats, Luca Marotti, Steffen Wollstadt, Rolf Scheiber
Microwaves and Radar Institute, German Aerospace Center, Germany

Abstract

This paper presents results on SAR interferometry with the so-called TOPS mode. The rationale to retrieve accurate interferometric products with such a mode is expounded, emphasizing the critical step of coregistering the pairs. Due to the particularities of the TOPS mode, a high Doppler-centroid is present at burst edges, demanding very high azimuth coregistration performance. A coregistration accuracy of one tenth of a pixel, as it is usually recommended with interferometric applications, will result in a large undesired azimuth phase ramp in the TOPS mode, above all at X-band. This paper presents two approaches based on the spectral diversity technique to estimate this offset with the required accuracy. Experimental results with repeat-pass TerraSAR-X data are shown to validate the proposed approach.

1 Introduction

TOPS (Terrain Observation by Progressive Scans) has been proposed as a new wide-swath imaging mode [1]. It overcomes the problems of scalloping and azimuth-varying signal-to-ambiguity ratio of the conventional ScanSAR mode by means of steering the antenna in the along-track direction. To achieve the same swath coverage and avoid the undesired effects of ScanSAR, the antenna is rotated throughout the acquisition from backward to forward at a constant rotation rate k_ϑ (see Fig. 1), opposite to the spotlight case. The fast steering leads to a reduction of the observation time, and consequently a worsening of the azimuth resolution. However, now all targets are observed by the complete azimuth antenna pattern, and therefore the scalloping effect diminishes and the azimuth ambiguities and the signal-to-noise ratio become constant in azimuth. At the end of the burst, the antenna look angle is changed to illuminate a second subswath, pointing again backwards. When the last subswath is imaged, the antenna points back to the first subswath, so that no gaps are left between bursts of the same subswath.

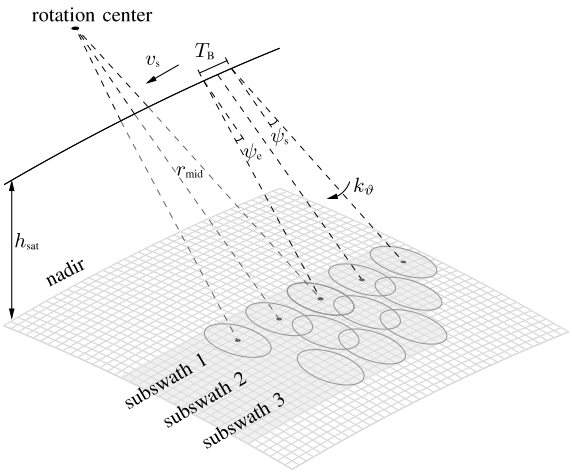

Figure 1: Sketch of the TOPS acquisition geometry.

Fig. 2 shows the time-frequency diagram (TFD) of one TOPS burst. The total azimuth bandwidth spans several PRF intervals, as in the spotlight case. Note also, that the rotation center is located behind the sensor, and as it happens in the ScanSAR mode, the focused burst is much larger than the raw data burst, requiring special care when performing the azimuth focusing. Note in Fig. 2 the dependence of the Doppler centroid on the azimuth position of the target within a burst, whose variation can reach several PRF intervals (the PRF is the gray area for a given time instant).

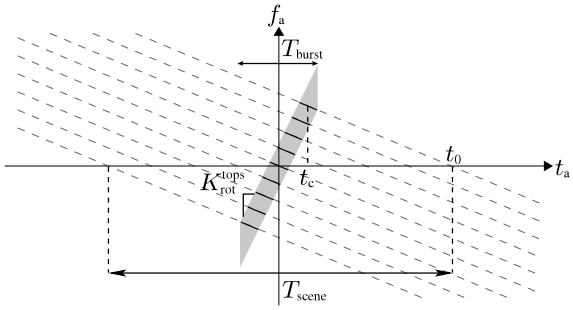

Figure 2: Time frequency diagram in the TOPS mode.

2 TOPS Processing

In order to retrieve accurate interferometric products, a phase-preserving processor is necessary. Baseband azimuth scaling (BAS) has been proposed as an efficient phase-preserving processor for the TOPS imaging mode, as well as being suitable for sliding-spotlight and ScanSAR [2]. The so-called extended chirp scaling (ECS) [3] is used for the range-variant processing, while BAS is used for the efficient focusing of the azimuth signal. In order to accommodate for the signal azimuth bandwidth, which in the TOPS mode is larger than the system PRF, a sub-aperture processing is performed, so that the sub-aperture bandwidth fits within the PRF. Afterwards, BAS is used

to perform the azimuth focusing in an efficient way, as the signal bandwidth still spans several times the PRF interval. Furthermore, the scene extension is larger than the raw data burst. BAS consists in a modified azimuth scaling approach, which solves these two problems simultaneously in an efficient way.

Table 1: Main System and Processing Parameters for the TOPS Acquisition

Wavelength	3.106 cm
# Swaths	4
# Bursts / swath	13
PRFs	4112 / 4030 / 4998 / 3897 Hz
Sampling frequency	109.88 MHz
Chirp bandwidth	100 MHz
Effective velocity	7392.58 m/s
Burst durations	0.23 / 0.25 /0.23 /0.27 s
Cycle time	1.005 s
Target Az. bandwidth	433 / 442 / 356 / 457 Hz
Range sampling	1.36m
Azimuth sampling	0.001551s ($\sim$ 11m)
Mid range	562 / 574 / 584 / 598 km
Rotation range	-94 / -105 / -96 / -124 km
Samples per burst	13 / 14 / 12 / 11 Ms
Samples in overlap area	1.2 / 1.6 / 3.6 / 1.8 Ms

3 TOPS Interferometry

3.1 Coregistration Accuracy Requirements

Similar as with ScanSAR, a precise knowledge of both the pointing accuracy and the along-track position are necessary in order to retrieve an interferometric pair with overlapping spectra [4]. However, one of the most challenging aspects in TOPS interferometry is the fact that the acquired data have large Doppler-centroid variations within a burst. For typical TerraSAR-X TOPS acquisitions, the Doppler centroid can vary by more than 7 kHz within one burst. It is well known that in presence of squint, linear phase ramps are induced in the focused response both in azimuth and range [5, 6]. Thus, constant misregistration can cause the presence of along-track and across-track linear phase ramps, of which the latter is in most cases negligible. However, since each TOPS burst is acquired with a varying Doppler centroid every focused point presents a different linear phase ramp in the azimuth direction. The slope of the ramp depends on the Doppler centroid. The resulting interferometric TOPS phase bias in the presence of azimuth misregistration is similar to the ScanSAR bias and is equal to [6]

$$\phi_{\text{azerr}} = 2\pi f_{\text{DC}} \Delta t, \tag{1}$$

where f_{DC} is the Doppler-centroid and Δt is the coregistration error in seconds. Within a burst, this corresponds to a linear phase term along azimuth, since f_{DC} is a function of the azimuth position within the burst. For a TerraSAR-X acquisition as given in Table 1, the Doppler variation reaches 5.4kHz. With the given image sampling, a misregistration of 0.1 pixel spacing introduces a ramp of approximately 1.6π within the burst. Therefore, an overall azimuth coregistration accuracy better than 0.001 of the pixel spacing is required for this configuration in order to achieve an error smaller than 3°.

3.2 Fine Coregistration with Spectral Diversity

Note that the above requirement applies mainly to a constant coregistration offset for the whole burst, and the achievable relative coregistration accuracy can be much better than this requirement. First, a coregistration can be performed either using orbit's information and an external DEM, amplitude cross-correlation, or coherence maximization, all of which yield accuracies better or around one tenth of a pixel. Then a fine coregistration using spectral diversity [6] with a large number of looks (all available data) would result in the required fine accuracy. Two possibilities are foreseen: the use of spectral diversity within a burst, or the use of spectral diversity in the overlapping region between two consecutive TOPS bursts. In the latter case, the spectral separation is much larger than the separation within the signal bandwidth due to the azimuth steering, and consequently much higher accuracy can be obtained. The achievable accuracy in the estimation of the coregistration error with spectral diversity in image samples is given by [7]

$$\sigma_{\text{sd}} = \frac{\sqrt{2}\sigma_{\text{look}}}{2\pi\Delta f}\frac{1}{\text{dt}}, \tag{2}$$

where Δf is the separation between looks, dt is the image sampling in seconds, and σ_{look} is the phase standard deviation of one look given by [7]

$$\sigma_{\text{look}} = \frac{1}{\sqrt{2N/\alpha}}\sqrt{\frac{B}{b}}\frac{\sqrt{1-\gamma^2}}{\gamma}, \tag{3}$$

where B is the processed bandwidth for a single target, b is the look bandwidth, N is the number of averaged samples, γ is the interferometric coherence, and α is the oversampling factor. When using the first possibility, i.e. spectral diversity within one burst, it has been shown in [7] that when $b = B/3$ ($\Delta f = B - b$), eq. (2) approaches the Cramér-Rao bound in the estimation of the coregistration error. When using the second option, i.e. spectral diversity in the overlapping region between two consecutive bursts, in (3) $b = B$, since the whole bandwidth is used. The second difference lies in the spectral separation Δf in (2). It can be shown that the spectral separation for the same pixel in two consecutive bursts is equal to

$$\Delta f_{\text{ovl}} = \left| \frac{2v_{\text{eff}}^2}{\lambda \cdot (r_{\text{rot}} - r)} T_{\text{cycle}} \right|, \tag{4}$$

where v_{eff} is the effective velocity, r is the range distance, r_{rot} is the rotation range, i.e. distance from the sensor to the rotation center, and T_{cycle} is the cycle time of the TOPS acquisition.

Fig. 3 shows the expected performances for the two presented possibilities. The system and processing parameters shown in Table 1 have been used for that purpose. As expected, the accuracy obtained using the overlap area is better than using one burst, since the final accuracy improves inversely proportional to Δf, while only inversely proportional to the square root of the number of averaged samples. Nevertheless, the performance of both approaches is sufficient to estimate the desired value, even for very low coherence values. Note also, that the information of all bursts can be used to further increase the number of looks (factor ~ 7.2 for the data shown in Section 4), since the constant offset applies to the whole acquisition, provided an accurate burst alignment on the processors' side. Besides the better performance of the second approach, it has also the advantage that the looks are already available, i.e. only the overlapping area of the left and right burst interferograms needs to be combined to generate the spectral diversity phase. This saves computational load when compared to the first approach, where the looks need to be generated explicitely. On the other hand, this approach has an important drawback: due to the larger sensitivity, the spectral diversity phase is might be wrapped. The maximum coregistration error in pixels that can be measured without aliasing is $\Delta p_{\max} = 1/(\Delta f \cdot \mathrm{dt})$. Using (4) and the parameters of Table 1, for this particular case this value is equal to 0.12 pixels. Therefore, it must be ensured that the residual coregistration error is smaller than this value, since otherwise a wrapped (wrong) value will be estimated.

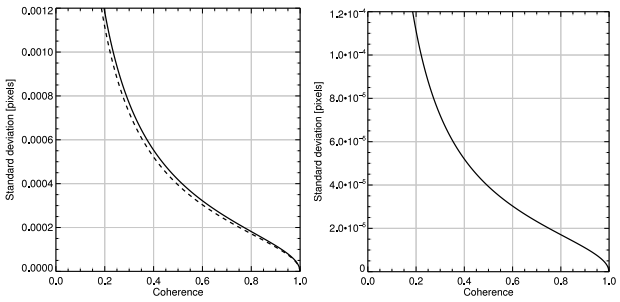

Figure 3: (left) Error in the estimation of the constant azimuth coregistration error within one burst for different coherence values (the dashed line shows the Cramér-Rao bound [7]), and (right) the same error when using the overlap area between consecutive bursts. The system and processing parameters of Table 1 have been used.

4 Experimental Results

Time series over Mexico City with the TOPS mode have been acquired by TerraSAR-X in both descending and ascending configurations. The ascending one has been acquired every cycle, i.e. every 11 days, while the descending one is interleaved with stripmap mode acquisitions, providing TOPS data every 22 days. Fig. 4 shows the TOPS reflectivity image of the descending configuration. The acquisition was commanded with four sub-swaths, thirteen bursts per sub-swath and an azimuth resolution of 16 m. Fig. 5 shows the coherence of a 22-day interferometric pair.

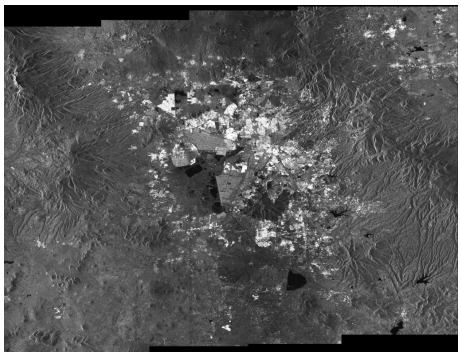

Figure 4: TOPS acquisition over Mexico City in a descending orbit configuration. Azimuth is vertical and range is horizontal, with near range on the left. Image dimensions: $\sim 100 \times 100$ km (ground-range).

Figure 5: Coherence over Mexico City with 22 days repeat-pass. The coherence ranges from 0 (black) to 1 (white).

4.1 Coregistration validation

In order to validate the achievement of the coregistration requirements, the third sub-swath of the Mexico City data take has been selected. Fig. 6 shows the interferometric phases after subtracting the SRTM DEM phase before and after the refined coregistration procedure (using one single burst). The coregistration error before is around 0.05 samples, corresponding to a 0.8π phase variation along each burst, which can be clearly identified, as well as the phase discontinuities between the bursts. After the refined coregistration, the phase ramps have vanished. The remaining

phase variations that can be observed are due to atmosphere, residual DEM errors, and deformation (see Section 4.2).

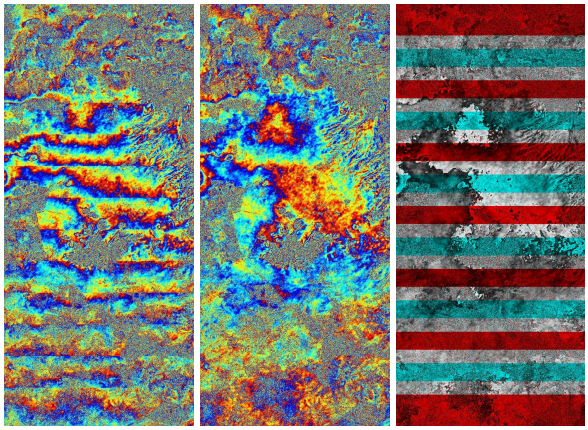

Figure 6: TOPS interferometric phase. (left) With a coregistration error of 0.05 samples. (middle) After using the first approach based on spectral diversity. The absolute azimuth coregistration error is better than 0.001 samples. (right) RGB representation where the phase of the odd bursts is in the red channel, and of the even bursts in the green and blue channels. The overlap areas appear mainly gray, hence proving no phase ramps are present.

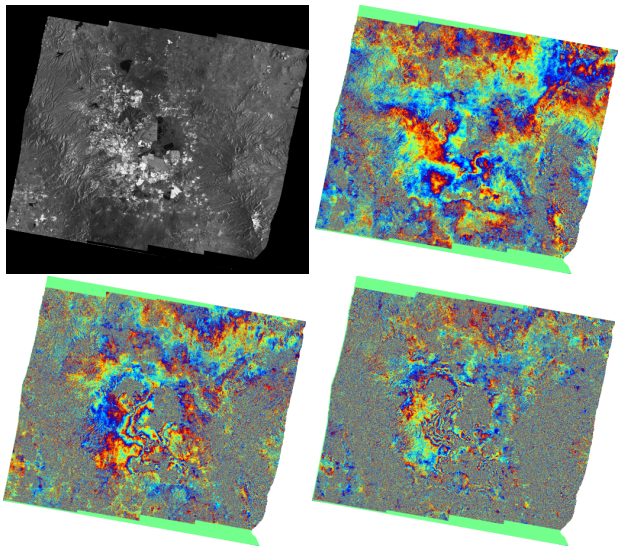

Figure 7: Geocoded reflectivity image together with three TOPS differential interferograms over Mexico City . The time-baselines are 22, 66 and 154 days.

4.2 DInSAR Results

Fig. 7 shows three geocoded TOPS differential interferograms over Mexico City with different time-baselines (SRTM was used to remove the topography), ranging from 22 days to 5 months. The increase in the number of fringes over a large part of the city area clearly shows the subsidence problem due to groundwater extraction [8]. Note that at X-band every fringe corresponds to 1.5cm of deformation in line-of-sight. No undesired phase ramps can be observed in the interferograms, confirming the validity of the proposed approach, and showing that it performs satisfactorily even with long-term pairs.

5 Conclusion

This paper has presented special investigations concerning the coregistration requirements in the TOPS mode. Due to the high Doppler variation within a burst, a very precise azimuth coregistration is needed. Two options to achieve the requirements have been presented, namely the use of spectral diversity either within a burst or between consecutive bursts. In both cases, the required performance can be achieved, since only a constant offset needs to be estimated and consequently a large number of samples can be averaged. Results with TerraSAR-X data have been presented to validate the proposed approaches. Further work will include the study of point-like scatterers to measure the residual coregistration error.

Acknowledgments

Work partially funded under ESTEC contract no. 22243/09/NL/JA.

References

[1] F. De Zan *et al.*: *TOPSAR: Terrain Observation by Progressive Scans*, IEEE Trans. Geosci. Remote Sensing, 44 (9), Sep. 2006.

[2] P. Prats *et al.*: *Processing of Sliding Spotlight and TOPS SAR Data Using Baseband Azimuth Scaling*, IEEE Trans. Geosci. Remote Sensing, 48 (2), Feb. 2010.

[3] A. Moreira *et al.*: *Extended Chirp Scaling Algorithm for Air- and Spaceborne SAR Data Processing in Stripmap and ScanSAR Imaging Modes*, IEEE Trans. Geosci. Remote Sensing, 34 (5), Sep. 1996.

[4] A. Meta *et al.*: *TOPS Imaging with TerraSAR-X: Mode Design and Performance Analysis*, IEEE Trans. Geosci. Remote Sensing, 48 (2), Feb. 2010.

[5] M. Bara *et al.*: *Interferometric SAR signal analysis in the presence of squint*, IEEE Trans. Geosci. Remote Sensing, 38 (5), pp. 2164-2178, Sep. 2000.

[6] R. Scheiber *et al.*: *Coregistration of interferometric SAR images using spectral diversity*, IEEE Trans. Geosci. Remote Sensing, 38 (5), pp. 2179-2191, Jul. 2000.

[7] R. Bamler *et al.*: *Accuracy of Differential Shift Estimation by Correlation and Split-Bandwidth Interferometry for Wideband and Delta-k SAR Systems*, IEEE Geosci. Remote Sensing Let., 2 (2), pp. 151-155, Apr. 2005.

[8] T. Strozzi *et al.*: *JERS SAR Interferometry for Land Subsidence Monitoring*, IEEE Trans. Geosci. Remote Sensing, 41 (7), pp. 1702-1708, Jul. 2003.